JOURNAL OF MATERIALS SCIENCE 30 (1995) 2153–2158

# The local structure characterization and resulting phase-transition mechanism of amorphous $ZrO_2$

ZENG YANWEI*
*Department of Materials Science and Engineering, Nanjing Institute of Chemical Technology, Nanjing 210009, People's Republic of China*
G. FAGHERAZZI, S. POLIZZI
*Department of Physical Chemistry, University of Venice, Venice 30123, Italy*

In the framework of Faber–Ziman's formalism, the radial atomic number density distributions $\rho(r)$ for two amorphous $ZrO_2$-gel samples have been derived, and used to perform local structure simulations based on the monoclinic and tetragonal crystal skeletons in order to determine and investigate the local structure of amorphous $ZrO_2$. The results indicate that the topological structure of amorphous $ZrO_2$ bears more resemblance to monoclinic $ZrO_2$ structure than to the tetragonal one. Moreover, the random structure in the amorphous $ZrO_2$ is characterized mainly by the first-kind disorder in the short-range. According to this structural picture of amorphous $ZrO_2$, a phase-transition mechanism of amorphous $ZrO_2$ has been proposed, by which the crystallization of amorphous $ZrO_2$ is considered starting with the formation of monoclinic nuclei followed by their further growth or conversion to the tetragonal phase, depending on the particular kinetic conditions and chemical environments. This proposed mechanism can help in the understanding of some experimental results that are not yet well understood.

## 1. Introduction

Zirconia, as a versatile ceramic material of great technical interest, has found a variety of applications due to its excellent properties in mechanics, electrics, optics etc. [1]. In recent years, some wet-chemical processes, especially alkoxide hydrolysis and sol–gel methods, appear to have enhanced research interest in $ZrO_2$ because of their unique advantages of achieving highly pure and homogeneous ultrafine $ZrO_2$ powders that can be utilized as well-qualified precursors for high-tech glass, ceramic coating, fibres, etc. [2, 3]. Moreover, the high surface area, fractal-porous texture, and good chemical durability possessed by ultrafine $ZrO_2$ powders make them a promising category of inorganic catalysts or catalyst supports, with potential applications in some important chemical synthesis industries [4–6].

It is well known that wet-chemical methods for the preparation of ultrafine $ZrO_2$ powder usually lead to amorphous products, despite some differences in the particular procedures. Amorphous $ZrO_2$ is structurally characterized by highly diffused humps in the wide-angle diffraction patterns at room temperature, and by a "glowing" phase-transition to monoclinic (m) and/or meta-stable tetragonal (t) phases during thermal treatment at temperatures around 400 °C, presumably depending on the details of the preparation procedure, such as the pH of the solution from which the amorphous $ZrO_2$ is obtained and the time taken to reach it [7, 8]. A significant phenomenon involved in the crystallization of amorphous $ZrO_2$ is the formation and metastability of tetragonal $ZrO_2$ at relatively low temperatures. The latter is often encountered in crystalline $ZrO_2$ powder and bulk materials. In order to understand the metastability of $ZrO_2$, many works have been devoted to the relevant studies, and various explanations for it have been proposed. Garvie [9, 10] advanced a surface energy argument, ascribing metastability of t-$ZrO_2$ to the lower surface energy of the tetragonal phase than that of the monoclinic phase, upon which a critical particle size, about 30 nm, was suggested as a criterion condition for the stabilization of t-phase. Mitshuashi *et al.* [11], however, claimed that the high lattice strain should be responsible for the metastability of polydomain t-$ZrO_2$ particles and that the existence of strain-free single-domain t-$ZrO_2$ particles is due to the absence of surface relief and a habit plane that are required for a martensitic transformation.

During the crystallization of amorphous $ZrO_2$, the t-$ZrO_2$ particles in the crystallization product are often simply considered to be directly formed and then stabilized due to the arguments mentioned above. A two-dimensional tetragonal-like structure model for amorphous $ZrO_2$ proposed by Livage *et al.* [12] seems to provide structural support for this. From Lavage *et al.*s model, Tani *et al.* [13] proposed a mechanism of topotactic crystallization of t-$ZrO_2$ on

* Author to whom all correspondence should be addressed.

0022–2461 

nuclei in amorphous $ZrO_2$, because the existence of tetragonal-like or quasi-t-$ZrO_2$ nuclei in amorphous $ZrO_2$ would certainly result in the formation of t-$ZrO_2$ phase. Nevertheless, such a crystallization mechanism for amorphous $ZrO_2$ frequently comes into conflict with experimental findings in the cases where the occurrence of monoclinic particles with diameters of about 10 nm (much smaller than Garvie's critical size) alone or together with tetragonal particles of a larger size than the coexisting monoclinic ones, has been found. Recently, a few investigators have made use of electron paramagnetic resonance spectroscopy to explore the influence of lattice defects on the formation and metastability of t-phase [14, 15]. Some results are indeed interesting, but the establishment of a direct correlation between lattice defects and the resulting products from phase transition in amorphous $ZrO_2$ still requires further attention.

In this paper, we present our novel insight into the local structure of amorphous $ZrO_2$, which was recently obtained through a topological structure simulation of the atomic number density distribution functions of amorphous $ZrO_2$ derived from wide-angle X-ray scattering (WAXS) intensity data by means of Fourier transform. Also, on this basis, we propose a mechanism for the phase transition occurring in amorphous $ZrO_2$ in an attempt to achieve a better understanding of this hitherto poorly understood phenomenon.

## 2. Local structure characterization

Generally, the initial crystallization product of an amorphous $ZrO_2$ would be associated with many physical and chemical factors. But the local structure of an amorphous $ZrO_2$ should be regarded as the most important factor, because it reflects all impacts from the employed wet-chemical process, and itself acts as the starting point of crystallization, in which the disorder–order transition will take place under the given conditions. Therefore, the elucidation of the local structure of amorphous $ZrO_2$ is supposed to be a key step to a full understanding of what happens with amorphous $ZrO_2$ during phase transition. Therefore, a careful WAXS study has been performed on two typical amorphous $ZrO_2$ samples in order to probe their local structures.

### 2.1. Amorphous $ZrO_2$ samples and WAXS measurements

The amorphous $ZrO_2$ samples used for WAXS studies include one $ZrO_2$ xerogel and one $ZrO_2$ aerogel, which are synthesized by different preparation procedures as concisely shown in Table I.

The WAXS measurements of the two samples were taken on the vertical scan X-ray diffractometer at room temperature. Filtered incident radiation was obtained, through a 1/2° divergent slit, from a molybdenum X-ray tube at 45 kV and 30 mA. The scattered beam, passing through a 0.2 m/m receiving slit, was collected in the step-scan mode at 0.05° intervals over an angular range from 10°–160° in 2θ, corresponding to the wavevector modulus ($h = 4\pi \sin(\theta)/\lambda$) from 15–175 $nm^{-1}$.

### 2.2. WAXS data analyses and discussion

In Fig. 1, two dotted lines designate the highly diffused WAXS patterns for $ZrO_2$ xerogel and aerogel samples, which are obtained from experimental scattering data after corrections for background, polarization, absorption, as well as normalization treatment by the high-angle method [16]. The solid lines indicate the theoretical coherent scattering intensity plus incoherent contribution $\langle |f(h)|^2 \rangle + I_{inc}(h)$. In order to reveal the local structure of amorphous $ZrO_2$, the WAXS data analyses were carried out in the framework of the Faber–Ziman formalism [17], by which the structure factor can be derived from the normalized coherent scattering intensity

$$S(h) = 1 + [I_{eu}(h) - \langle f^2(h) \rangle]/\langle f(h) \rangle^2 \quad (1)$$

and the pair-distribution function $G(r)$, is obtained from the following Fourier transform

$$G(r) = 4r(\rho - \rho_0) = 2/\pi \int_0^{h_{max}} \{S(h) - 1\} M(h) \sin(rh)\, dr \quad (2)$$

where $\langle\ \rangle$ represents a compositional average and $f(h)$ is the atomic form factor calculated in terms given by Cromer and Waber [18]; ρ is the atomic number

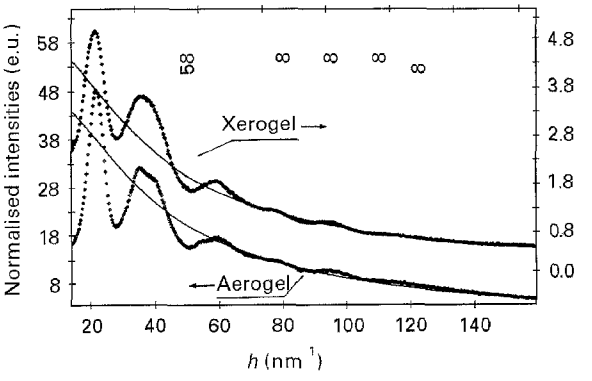


*Figure 1* Normalized WAXS diffraction intensities for $ZrO_2$-aerogel and xerogel.

TABLE I Synthesis procedures for $ZrO_2$ xerogel and aerogel

| Sample | $[H_2O]/[Zr(OC_3H_7)_4]$ | pH | Drying method | $A_s(m^2\ g^{-1})$ |
|---|---|---|---|---|
| $ZrO_2$ xerogel | 4.0 | 4.5 ($HNO_3$) | Under vacuum $10^{-2}$ torr, 25 °C | 113 |
| $ZrO_2$ aerogel | 15 | 9.5 ($NH_4OH$) | Supercritical (250 °C, 65 atm) | 381 |

density distribution function of the samples, and $\rho_0$ the average value of density, $\rho$, over the sample; $M(h) = \exp(-0.015h^2)$, a Gaussian type of convergence factor introduced into the above Fourier transform to suppress the spurious termination errors and eliminate the influence from the less accurate high-angle data; $h_{max}$ is the upper limit of the used wave-vector modulus.

Directly from Equation 2, the atomic number density distribution curves, $\rho(r)$ for $ZrO_2$ aerogel and xerogel samples were derived, with the results illustrated by dotted lines in Figs 2 and 3, respectively. For a simple structure comparison, the first peak positions determined from Fig. 2 are listed in Table II, together with the calculated Zr–O distances in crystalline $ZrO_2$s by a simple arithmetic average with reference to other sources [19, 20]. At first, it can be seen that the mean values of the nearest neighbour distances,

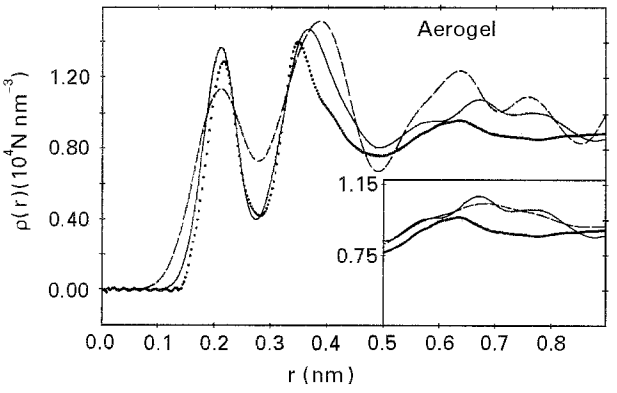


*Figure 2* Radial atomic number density distribution function for $ZrO_2$ aerogel: (···) experimental function, and those developed by the first-kind disorder models with (——) monoclinic and (– – –) tetragonal structures. The inset shows the result from (– – –) a para-crystalline monoclinic model versus (——) the first-kind model.

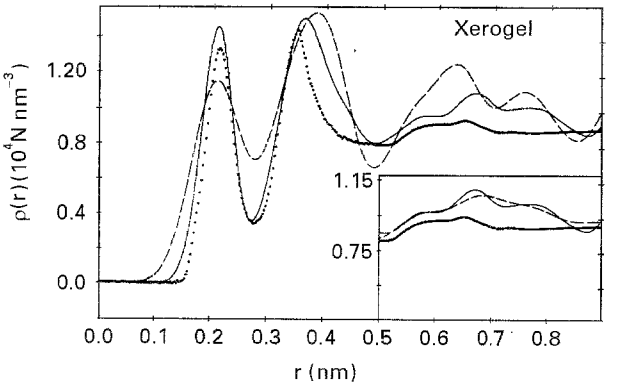


*Figure 3* Radial atomic number density distribution function for $ZrO_2$ xerogel. For key, see Fig. 2.

TABLE II Interatomic distances $ZrO_2$ xerogel, aerogel and crystalline $ZrO_2$

| Sample | Interatomic distance (nm) | |
|---|---|---|
| | $R_{Zr-O}$ | $R_{Zr-Zr}$ |
| Xerogel | 0.213 | 0.348 |
| Aerogel | 0.213 | 0.345 |
| t-$ZrO_2$ | 0.224 | 0.363 |
| m-$ZrO_2$ | 0.216 | 0.347 |

$R_{Zr-O}$, for two samples are exactly the same within the experimental accuracy, regardless of their differences in preparation procedures. This result seems to imply that different preparation methods makes little change in the local coordination bond-length of the amorphous $ZrO_2$ gels. On the other hand, the average distance $R_{Zr-O}$ and $R_{Zr-Zr}$ in $ZrO_2$ gels are quite close to those in monoclinic $ZrO_2$, but far from those in tetragonal $ZrO_2$. This fact suggests that the three-dimensionally averaged nearest coordination polyhedra $[ZrO_n]$ in the amorphous $ZrO_2$ are more like those in crystalline m-$ZrO_2$ than in t-$ZrO_2$. Nevertheless, it should be pointed out that such a simple comparison would not give a reliable conclusion as to whether or not there exists a local structural parallelism between the amorphous $ZrO_2$ and one of the crystalline $ZrO_2$s. A reliable conclusion about structural characteristics should be achieved at least through a full analysis of atomic number density distribution over a real-space range of interest, rather than a few peak positions. In amorphous materials, the interatomic distances do not assume a few discrete values as in the crystalline state. Instead, they usually show a distribution varying from one material to another, and depending on the preparation conditions for the materials of the same chemistry, although they may cover some of the interatomic distances present in crystalline counterparts. Therefore, the finding of some peak positions in the distribution function approximately equal to some interatomic bond-lengths in the crystalline state does not suffice to draw the conclusion that their structure is similar.

With the purpose of obtaining a full structural description of amorphous $ZrO_2$, a structure simulation, by incorporating the first-kind disorder and second-kind disorder into the tetragonal and monoclinic model structures, has been tried on the atomic number density distribution functions, $\rho(r)$. With the structural models of the first-kind disorder, the Equation 3 was used and the major simulation results for two samples are demonstrated in Figs 2 and 3, where the continuous and discontinuous lines, respectively, correspond to the uses of monoclinic and tetragonal models.

$$\rho'(r) = W_{ij}[\rho'_{ij}(r)/c_j]$$

$$\rho'_{ij}(r) = 1/\sigma_{ij}^2\pi\exp[-(r-r_{ij})^2/2\sigma_{ij}^2]/4\pi r^2 \quad (3)$$

where $r_{ij}$, the distance of the $j$th atom from the $i$th atom located at a reference centre, is determined by the selected crystallographic lattices (tetragonal or monoclinic $ZrO_2$); $\sigma_{ij}$, the standard mean square deviation representive of the magnitude of structural disorderness, is adjusted as a refinable parameter during the simulating process towards the minimization of the residual errors $|\rho(r) - \rho'(r)|^2$; and the weighting factor $W_{ij} = f_i f_j c_i c_j / \langle f^2 \rangle$ is used in its averaged value over the diffraction range of this study.

As seen from Fig. 2, the monoclinic structural model provides a much better simulation to the experimental density curves for both $ZrO_2$ xerogel and aerogel samples than does the tetragonal model. The former produces an excellent fit, both in both peak position and peak profile, to the experimental density,

$\rho(r)$, in the first peak range, while the latter results in rather broad and lower peaks than the experimental ones, although they reach their maxima at almost the same $r$ values as in the former case. Starting from the second peak, the calculated density curves for the tetragonal model exhibit a large amplitude of oscillations around the experimental density curves. In contrast, the monoclinic-lattice-derived density curves still keep in pace with the experimental ones, despite an evident deviation from the experimental curves occurring after $r = 0.35$ nm. Obviously, such a deviation may be partially ascribed to the smallness of the $ZrO_2$-gel particles in respect to the model size, because the presence of a large quantity of surface phase will necessarily reduce the percentage of long-distance atom pairs. Additionally, the existence of second-kind disorder in amorphous $ZrO_2$ should also be responsible for this deviation. To consider this, a paracrystalline model [21] was used in the high $r$ range (beyond 0.5 nm), where the standard deviation, $\sigma_{ij}$, is supposed to be a function of distance $r$

$$\sigma_{ij} = K_{ij} r^{1/2} \tag{4}$$

As shown in the insets of Figs 2 and 3, the paracrystalline model gave a $\rho'(r)$ function (---) closer in shape to the experimental ones. This improvement implies that the first-kind disorder prevails in the short-range, while the second-kind disorder should be involved when the radius, $r$, reaches a certain large value.

From the structure simulation results above, it can be summarized that, in the amorphous $ZrO_2$, the atoms are indeed not arranged in a completely random manner, as implied in Livage *et al.*'s model. However, the topological structure could be characterized mainly by a monoclinic $ZrO_2$ lattice plus the first-kind disorder alone in the short-range, as well as the second-kind disorder when the pair-interatomic distance, $r$, amounts to a certain large value. Thus, the local structure of amorphous $ZrO_2$ may be approximately considered to be equivalent to a crystal monoclinic lattice modulated by an appropriate first-kind disorder, even far beyond the nearest neighbour coordination shell. Such a structural picture of amorphous $ZrO_2$ allows us to conclude that amorphous $ZrO_2$ possesses a partially ordered short-range structure, which bears a greater resemblance to crystalline monoclinic $ZrO_2$ than to the tetragonal form. This conclusion could also be supported by local structural symmetry. The monoclinic $ZrO_2$ has the lowest rotation symmetry of the three polymorphs of crystalline $ZrO_2$. Therefore, if there is a certain ordered short-range structure in amorphous $ZrO_2$, it should be lower in rotation symmetry than the monoclinic form and much lower than the tetragonal $ZrO_2$. Consequently, it is physically reasonable to consider the short-range structure in amorphous $ZrO_2$ to be more similar to monoclinic $ZrO_2$ than to the tetragonal form.

## 3. Phase-transition mechanism

In general, a particular mechanism for a real dynamic process in company with structure change is closely associated with the structural relationship before and after the process. The initial structure governs the route by which the dynamic process starts to proceed. This is at least the case in the initial stage of a dynamic process. Also, from the viewpoint of energy, a spontaneous dynamic process must follow the direction leading the system to a decrease in total energy. Undoubtedly, these general laws are helpful in the analysis of the phase-transition mechanism for amorphous $ZrO_2$.

In view of the structure simulation results, the local atomic structure of amorphous $ZrO_2$ is characterized by a monoclinic symmetry modulated by a large first-kind disorder. Certainly, such a structural feature allows it to be inferred that monoclinic $ZrO_2$ nuclei would be more easily formed than other phases through a topotactic rearrangement at the onset of the crystallization. As a result, small monoclinic crystallites or crystalloids would be first formed from the crystallization of amorphous $ZrO_2$. Moreover, because the major local structural features in the amorphous $ZrO_2$ are differentiated from those in monoclinic $ZrO_2$ only by the first-kind disorderliness, the topotactic rearrangement can be expected to be thermally activated at comparatively low temperatures; and once thermally activated, this process could take place very rapidly. Obviously, this inference can give a good interpretation of the fact that the phase transition of amorphous $ZrO_2$ derived from wet-chemical methods often occurs sharply at temperatures as low as around 400 °C.

As the monoclinic $ZrO_2$ nuclei are formed, however, how the subsequent dynamic processes will proceed is expected to be controlled by both thermodynamic and kinetic factors. From the viewpoint of thermodynamics, the interfacial effects may have an impact on the subsequent dynamic process, which is supposed to include the interfacial energy differences between monoclinic and other $ZrO_2$ polymorphs, determined by their surface structural difference (intrinsic property), and the local chemical environments in which the m-$ZrO_2$ nuclei exist (extrinsic influence). It should be noted that the local chemical environment with which the fresh m-$ZrO_2$ nuclei are directly in contact, may differ greatly from the macro-scalar surroundings. For instance, the foreign substances removed from the structure due to the crystallization of amorphous $ZrO_2$ would eventually constitute part of the local chemical environment, even though the samples are apparently treated in a homogeneous medium. Generally, therefore, three different possibilities exist, which are likely to occur subsequently with the freshly created monoclinic $ZrO_2$ nuclei.

One of the possibilities corresponds to a higher interfacial energy of monoclinic $ZrO_2$ micro-grains than to tetragonal ones, as argued by Garvie [9, 10]. In this case, a diffusionless phase transition from the monoclinic nuclei to tetragonal phase would be expected to occur from the viewpoint of thermodynamics. In addition, this transition would probably take place in those growing monoclinic particles that are formed by further growth of monoclinic nuclei. As a result, tetragonal $ZrO_2$ grains must be found in the

final crystallization products, and the t-phase grains formed in this way are expected to contain more or less internal strain caused during the m → t phase-transition process, depending on the details of intra-particle structure.

The second possibility may be the single further growth of tiny monoclinic $ZrO_2$ nuclei corresponding to a lower interfacial energy of monoclinic $ZrO_2$ than other $ZrO_2$ polymorphs. Thermodynamically, this process can be driven by the decrease in total surface area of the crystallites. Although this possibility, contrary to Garvie's hypothesis, has not yet been found in literature, it is a quite plausible circumstance, because varying local chemical environments around tiny nuclei of m-$ZrO_2$ might change the relative magnitude of their surface energies (especially in those liquid media with a multiple species of ions). Obviously, this case makes it possible to observe experimentally the pure monoclinic $ZrO_2$ particles as crystallization products.

The last possibility corresponds to the case where the monoclinic and tetragonal $ZrO_2$ particles possess an appropriate surface energy difference ($\sigma_m - \sigma_t = r/3[g_t - g_m]$, where $\sigma$ refers to the surface free energy, $g$ to the free energy/unit volume of $ZrO_2$ of "infinite" size, $r$ the particles radius), so that the newly formed m-phase tiny nuclei or particles cannot obtain a sufficiently high thermodynamical driving force to transform into tetragonal ones. As a consequence, as in the case of the second possibility, the monoclinic $ZrO_2$ particles are expected to be observed in reality.

By reference to the above-mentioned three possibilities for newly-formed monoclinic $ZrO_2$ phase, a schematic energy-state diagram can be worked out, as shown in Fig. 4 for each case. It should be emphasized that here the crystallization of amorphous $ZrO_2$ is considered, starting with the formation of monoclinic $ZrO_2$ nuclei due to the local structure resemblance between monoclinic and amorphous $ZrO_2$. From Fig. 4a, it can be seen that the transition of newly formed monoclinic $ZrO_2$ nuclei to tetragonal ones is thermodynamically driven by $G_1$, and at the same time kinetically dominated by the energy-barrier height, $G_2$, which is expected to determine the extent to which the newly-formed monoclinic nuclei transform to tetragonal ones within a given experimental time. As shown in Fig. 4b, the m–t transition free-energy, $G_1$, is opposite in sign to that of case 1, so that only m-phase can be found because the m–t transition is thermodynamically prohibited. For case 3, see Fig. 4c, the energy barrier height between m- and t-phases at the same energy levels is also designated $G_2$, which prevents the newly formed m-phase nuclei from transforming to tetragonal phase. But, in practice more or less m–t transition is expected to occur if the energy fluctuation is present. Therefore, this case may correspond to the little or trace existence of tetragonal phase, together with monoclinic phase in large quantity.

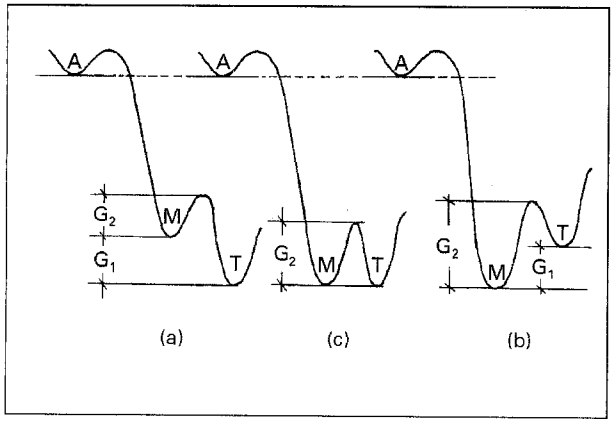


*Figure 4* Schematic diagram of free-energy states corresponding to three thermodynamic possibilities for newly formed monoclinic $ZrO_2$ phase.

To sum up the above discussions, the following possible plot of the mechanism of the phase transition of amorphous $ZrO_2$ can be drawn.

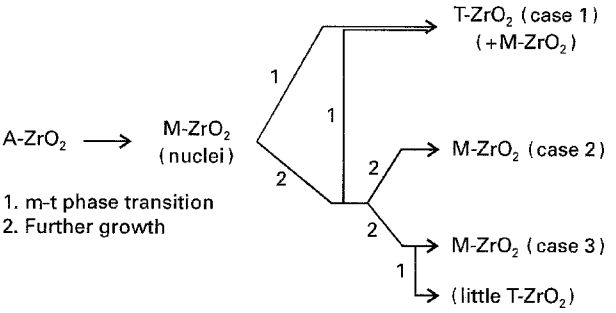


The important advantage in the present phase-transition mechanism lies in that it enables some experimental results that were formerly not well understood, to be elucidated. For instance, it can explain why the frequent occurrence of monoclinic $ZrO_2$ of small size, alone or together with tetragonal $ZrO_2$ of larger size than the coexisting monoclinic $ZrO_2$ have been observed. In fact, if the topotactic crystallization of t-$ZrO_2$ in amorphous $ZrO_2$ is true, it is not possible to find the m-phase grains smaller than the critical size according to Garvie's argument, because t-$ZrO_2$ undergoes a t → m transition only when it grows to above its critical size. Using the as-proposed mechanism, the occurrence of monoclinic $ZrO_2$ particles, alone or together with larger tetragonal $ZrO_2$ ones, could be naturally thought of as a possible result of kinetic competition and/or compromise between m → t transition and further growth of newly formed m-$ZrO_2$ in a given experimental time, which are both thermodynamically allowable and associated with the energy barrier height between the m- and t-phase, as in Fig. 4a and c. In addition, if the first formation of t-$ZrO_2$ is true, it is easy to imagine that either poly- or single-domain t-phase particles grown from their green bodies should be strain-free for ultrafine $ZrO_2$ powders derived by wet-chemical methods, because there is no good reason why some mechanical restrictions could be involved in such a process. However, this seems in contradiction with the real cases where tetragonal particles often possess some degree of internal microstrain. In fact, from the as-proposed mechanism, the micro-strain present in those polydomain

tetragonal particles may be interpreted as the consequence of the m → t transition, depending on the details of domain structure and size. Therefore, the attribution of the existence of tetragonal $ZrO_2$ in ultrafine $ZrO_2$ powder to domain-boundary inhibition from the t → m transition seems unreasonable in powder systems. In addition, it may not be logical to take this fact as support for the above attribution that the almost pure tetragonal $ZrO_2$ powders are found to have the largest lattice-strain [11].

## 4. Conclusions

The local structure simulations carried out on the atomic number density distributions of two amorphous $ZrO_2$ samples indicate that the topological structure of the amorphous $ZrO_2$ bears more similarity to the monoclinic $ZrO_2$ structure than it does to the tetragonal one. Moreover, the structural randomness in the amorphous $ZrO_2$ is characterized mainly by the first-kind disorder alone, in the short-range, but also with the second-kind disorder when the pair-interatomic distance, $r$, increases to a certain large value. From this structural picture of amorphous $ZrO_2$, the crystallization of amorphous $ZrO_2$ is considered to begin with the formation of monoclinic nuclei followed by their further growth and/or transition to the tetragonal phase, depending on the particular kinetic conditions and chemical environments in which the monoclinic nuclei were formed. This proposed mechanism can be used to explain experimental results which have hitherto remained poorly understood.

## References


1. A. H. HEUER and L. W. HOBBS, "Advances in Ceramics", Vol. 3 (American Ceramic Society, Columbus, OH, 1981).
2. D. GARGNLI and D. KUNDER, *J. Mater. Sci. Lett.* **3** (1984) 503.
3. L. L. HENCH and D. R. ULRICH, "Ultrastructure Processing of Ceramics, Glasses and Composites" (Wiley-Interscience, New York, 1984).
4. B. DENISE and R. P. A. SNEEDEN, *Appl. Catal.* **28** (1986) 235.
5. Y. AMENOMIYA, *ibid.* **30** (1987) 57.
6. Y. AMENOMIYA and I. T. ALIEMESH in, "Proceedings of the 9th International Congress on Catalysis", Calgary, Vol. 2 (1988) p. 634.
7. R. SRINIVASAN and R. DE ANGELIS, *et al.*, *J. Mater. Res.* **1** (1986) 583.
8. R. SRINIVASAN, M. B. HARRIS, S. F. SIMPSON, R. J. ANGELIS and B. H. DAVIS *ibid.* **3** (4) (1988) 787.
9. R. C. GARVIE, *J. Phys. Chem.* **69** (1965) 1230.
10. *Idem, ibid.* **82** (1978) 218.
11. T. MITSHUASHI, M. ICHIHARA and V. TATSUKE, *J. Am. Ceram. Soc.* **57** (1974) 97.
12. J. LIVAGE, K. DOI and C. MAZERES, *J. Am. Ceram. Soc.* **51** (1968) 349.
13. E. TANI, M. YOSHIMURA and S. SŌMIYA, *ibid.* **66**(3) (1983) 11.
14. M. J. TORRALVO, M. A. ALARIO and J. SORIA, *J. Catal.* **86** (1984) 473.
15. M. I. SENDI, J. S. MOYA, C. J. SERNA and J. SORIA, *J. Am. Ceram. Soc.* **68**(3) (1985) 135.
16. G. S. CARGILL III, "Solid State Physics", Vol. 3 (Academic Press, New York, 1975) p. 227.
17. T. E. FABER and J. M. ZIMAN, *Philos. Mag.* **11** (1965) 153.
18. D. T. CROMER and J. T. WABER, *Acta Crystallogr.* **18** (1965) 104.
19. G. TEUFER, *ibid.* **15** (1962) 1187.
20. D. K. SMITH and H. W. NEWKIRK, *ibid.* **18** (1965) 983.
21. R. HOSEMANN and S. N. BAGCHI, "Direct Analysis of Diffraction by Matter" (North-Holland, Amsterdam, 1962).



*Received 13 May 1993*
*and accepted 8 September 1994*